PIAS1 modulates striatal transcription, DNA damage repair, and SUMOylation with relevance to Huntington's disease

Eva L. Morozko[a,1], Charlene Smith-Geater[b,1], Alejandro Mas Monteys[c], Subrata Pradhan[d], Ryan G. Lim[e], Peter Langfelder[f], Marketta Kachemov[a], Austin Hill[g], Jennifer T. Stocksdale[a], Pieter R. Cullis[h,i], Jie Wu[j], Joseph Ochaba[a], Ricardo Miramontes[e], Anirban Chakraborty[k], Tapas K. Hazra[k], Alice Lau[b], Sophie St-cyr[c], Iliana Orellana[l], Lexi Kopan[b], Keona Q. Wang[b], Sylvia Yeung[e], Blair R. Leavitt[m], Jack C. Reidling[e], X. William Yang[n], Joan S. Steffan[b,e], Beverly L. Davidson[c,o,2], Partha S. Sarkar[d,p,2], and Leslie M. Thompson[a,b,e,j,l,2,3]

[a]Department of Neurobiology and Behavior, University of California, Irvine, CA 92697; [b]Department of Psychiatry and Human Behavior, University of California, Irvine, CA 92697; [c]Raymond G. Perelman Center for Cell and Molecular Therapeutics, The Children's Hospital of Philadelphia, Philadelphia, PA 19104; [d]Department of Neurology, University of Texas Medical Branch, Galveston, TX 77555; [e]Institute of Memory Impairments and Neurological Disorders, University of California, Irvine, CA 92697; [f]Department of Human Genetics, David Geffen School of Medicine at University of California, Los Angeles, CA 90095; [g]Incisive Genetics Inc., Vancouver, BC, Canada V6A 0H9; [h]NanoMedicines Innovation Network, University of British Columbia, Vancouver, BC, Canada V6T 1Z3; [i]Department of Biochemistry and Molecular Biology, University of British Columbia, Vancouver, BC, Canada V6T 1Z3; [j]Department of Biological Chemistry, University of California, Irvine, CA 92697; [k]Department of Internal Medicine, University of Texas Medical Branch, Galveston, TX 77555; [l]Sue and Bill Gross Stem Cell Institute, University of California, Irvine, CA 92697; [m]Centre for Molecular Medicine and Therapeutics, University of British Columbia, Vancouver, BC, Canada V5Z 4H4; [n]Center for Neurobehavioral Genetics, Semel Institute for Neuroscience and Human Behavior, University of California, Los Angeles, CA 90095; [o]Department of Pathology and Laboratory Medicine, University of Pennsylvania, Philadelphia, PA 19104; and [p]Department of Neuroscience and Cell Biology, University of Texas Medical Branch, Galveston, TX 77555

Edited by Stephen T. Warren, Emory University School of Medicine, Atlanta, GA, and approved December 14, 2020 (received for review October 26, 2020)

DNA damage repair genes are modifiers of disease onset in Huntington's disease (HD), but how this process intersects with associated disease pathways remains unclear. Here we evaluated the mechanistic contributions of protein inhibitor of activated STAT-1 (PIAS1) in HD mice and HD patient-derived induced pluripotent stem cells (iPSCs) and find a link between PIAS1 and DNA damage repair pathways. We show that PIAS1 is a component of the transcription-coupled repair complex, that includes the DNA damage end processing enzyme polynucleotide kinase-phosphatase (PNKP), and that PIAS1 is a SUMO E3 ligase for PNKP. Pias1 knockdown (KD) in HD mice had a normalizing effect on HD transcriptional dysregulation associated with synaptic function and disease-associated transcriptional coexpression modules enriched for DNA damage repair mechanisms as did reduction of PIAS1 in HD iPSC-derived neurons. KD also restored mutant HTT-perturbed enzymatic activity of PNKP and modulated genomic integrity of several transcriptionally normalized genes. The findings here now link SUMO modifying machinery to DNA damage repair responses and transcriptional modulation in neurodegenerative disease.

DNA damage repair | SUMO | PIAS | Huntington's disease | PNKP

Huntington's disease (HD) is a devastating genetic neurodegenerative disease caused by an expanded CAG repeat within the HD gene (*HTT*), which is translated into an expanded polyglutamine (PolyQ) repeat within the Huntingtin (HTT) protein (1, 2). The size of the repeat expansion inversely correlates with age of onset in HD patients, with CAG-repeat length accounting for about 50% of the observed age of onset (2, 3). Genetic variants in DNA damage repair (DDR) genes, such as FANCD2/FANCI-associated nuclease 1 (*FAN1*) and MutS homolog 3 component of MutS beta (*MSH3*), have been identified that contribute to variation in age of onset (4–7).

Posttranslational modifications, including small ubiquitin-like modifier (SUMO) modification, are integral signaling components that participate in numerous cellular processes (8, 9). For DDR, SUMO modulates localization and protein degradation of repair components with dysregulation leading to genomic instability and diseases (10). Dysregulation of SUMOylation is associated with neurodegenerative diseases including HD and other CAG-repeat disorders, Parkinson's disease (PD), and Alzheimer's disease (AD) (9, 11–13). We previously demonstrated that the HTT protein is SUMO modified (14) and identified Protein Inhibitor of Activated STAT-1 (PIAS1) as an E3 SUMO ligase that enhances SUMOylation of HTT (15). Viral miRNA-mediated knockdown (KD) of Pias1 in R6/2 striata improved behavior and molecular readouts associated with HD progression (16). However, the precise mechanisms affected by PIAS1 in HD are not yet defined, nor is the role of PIAS1 in neurons known.

Here we evaluated the consequences of Pias1 reduction in a HD knockin mouse model which expresses the human expanded

Significance

Genetic variants in genes involved in maintenance of genomic stability are modifiers of Huntington's disease (HD) age of onset. This study shows a connection between the E3 SUMO ligase PIAS1, DNA damage repair protein PNKP, and HD-associated transcriptional dysregulation. Reduction of Pias1 in a knockin HD mouse striatum normalizes disease-associated aberrant transcription, rescues perturbed enzymatic activity of Pnkp, and increases genomic integrity, while also having transcriptional effects in WT animals. PIAS1 reduction in human iPSC neurons alters transcription of synaptic signaling and DNA damage repair, rescues PNKP activity, and increases genomic integrity in HD iPSC-derived neurons. Finally, PIAS1 can modulate SUMO modification of PNKP, which is the first identification of an enzyme that regulates this modification.

Author contributions: E.L.M., C.S-G., A.M.M., B.R.L., J.C.R., B.L.D., P.S.S., and L.M.T. designed research; E.L.M., C.S-G., A.M.M., S.P., M.K., A.H., J.T.S., P.R.C., J.O., A.C., T.K.H., A.L., S.S.-c., I.O., L.K., K.Q.W., and S.Y. performed research; E.L.M., C.S.-G., S.P., R.G.L., P.L., J.W., R.M., J.C.R., X.W.Y., and J.S.S. analyzed data; E.L.M., C.S.-G., J.C.R., X.W.Y., J.S.S., and L.M.T. wrote the paper; and B.L.D., P.S.S., and L.M.T. provided resources and funding acquisition.

The authors declare no competing interest.

This article is a PNAS Direct Submission.

[1]E.L.M. and C.S.-G. contributed equally to this work.

[2]B.L.D., P.S.S., and L.M.T. contributed equally to this work.

[3]To whom correspondence may be addressed. Email: lmthomps@uci.edu.

This article contains supporting information online at https://www.pnas.org/lookup/suppl/doi:10.1073/pnas.2021836118/-/DCSupplemental.

Published January 18, 2021.

repeat region encoded by exon 1 within the endogenous murine *Htt* locus, producing a chimeric full-length, mutant HTT (mHTT) protein (17). Heterozygous zQ175 mice have subtle disease phenotypes and Pias1 KD did not significantly alter their behavior. Assessment of molecular phenotypes revealed significant effects of Pias1 reduction. Bulk mRNAseq analysis revealed that Pias1 KD modulates transcriptional readouts in both WT and HD mice. A subset of specific HD-associated transcriptional profiles were normalized with presymptomatic Pias1 KD; specifically, in genes enriched for processes involved in neuronal and synaptic function. Compared to established transcriptional modules of a zQ175 allelic series (18), presymptomatic Pias1 KD also rescued disease-associated DDR-related modules, suggesting that Pias1 may regulate repair pathways in vivo. PIAS1 KD in control and patient-derived induced pluripotent stem cells (iPSCs) differentiated into medium spiny neurons (MSNs) showed a similar effect on synaptic terms and DDR.

We previously showed that transcription-coupled repair (TCR) is impaired in HD models, with the HTT protein itself serving as a scaffold for the TCR complex (19). HTT is also involved in base-excision repair (BER) (20). In HD model systems, the presence of mHTT results in decreased enzymatic end-processing activity of the DNA repair protein, polynucleotide kinase 3′-phosphatase (PNKP) (19), a component of the BER and TCR pathways (21, 22). Therefore, mHTT expression may directly impact DDR mechanisms. Of relevance, PIAS1 contributes to DDR pathways as a SUMO E3 ligase, potentially to recruit repair factors (23) or mark them for eviction or clearance (24).

Given the findings above, we investigated whether PIAS1 modulates repair activity in zQ175 mice and in HD iPSC-derived MSNs by assessing PNKP enzymatic activity and genomic integrity of several transcriptionally modulated genes. We show that PIAS1 KD rescued PNKP activity in zQ175 mouse striatum and HD MSNs, with a corresponding increase in genomic stability of several target genes transcriptionally modulated by Pias1 in zQ175 mice. Further, PIAS1 acts as a SUMO E3 ligase for PNKP in cells. Our data supports a role for SUMOylation in modulating neuronal homeostasis in neurodegenerative disease and defines PIAS1 as a key component of a DDR pathway in neurons. Therefore, PIAS1 may be serving as a modulatory component of TCR and as a regulator of transcriptional networks associated with repair processes and neuronal function in the context of HD.

Results

Characterization of Symptomatic and Presymptomatic Pias1 KD in zQ175 Mice. To reduce Pias1 in a slowly progressing HD mouse, we used heterozygous zQ175 knockin mice which exhibit subtle behavioral deficits starting around 7 months of age (mo) (17). For this study, we designated 2.5 mo as "presymptomatic" and 7.5 mo as "symptomatic" (*SI Appendix*, Fig. S1*A*). Accumulation of high molecular weight (HMW) mHTT is also detectable after 6 mo and increases over time (*SI Appendix*, Fig. S1 *B–D*). Male and female heterozygous (Het/zQ175) or wild-type (WT) littermates were treated with AAV2/1 expressing either a miRNA against Pias1 (miPias1.3), a control scrambled miRNA (miSafe), or a vehicle control (saline) through bilateral stereotaxic striatal injections as described (16). GFP is coexpressed as a viral reporter and can be detected 11 mo after injection (*SI Appendix*, Fig. S1*E*). Behavioral analysis is described in detail in *SI Appendix* and outcomes provided in *SI Appendix*, Figs. S2 and S3; statistical outputs are detailed in Dataset S1. Overall, animals exhibited minimal genotype-related behavioral deficits as described (17, 25) with little to no further impact observed by miPias1.3 treatment.

KD efficiency was assessed by measuring Pias1 transcript levels from GFP-positive microdissected striata at 13.5 mo, a month after behavioral analysis as no additional behavioral changes are observed in zQ175 mice between 12 and 15 mo (26). Significant KD of Pias1 transcript was observed at 13.5 mo by qPCR for both males and females in symptomatic (*SI Appendix*, Fig. S4 *A* and *D*) and presymptomatic mice (*SI Appendix*, Fig. S5 *A* and *D*). No differences in Pias1 protein levels were detected in either WT or zQ175 mice at this age in either insoluble or soluble fractions (15, 16) for most groups with the exception of symptomatic-treated females in the soluble fraction (*SI Appendix*, Figs. S4*F* and S5).

Since Pias1 KD at 13.5 mo showed successful reduction of Pias1 at the transcript level, but little to no difference at the protein level, we assessed KD efficiency in striata at an earlier time point of 8 mo, just after symptomatic onset, following presymptomatic KD injections at 2.5 mo (17). A small cohort of animals was used specifically to evaluate biochemical and molecular readouts. Behavior was performed for enrichment (27) and consistency with the longer-term studies (Dataset S1 and *SI Appendix*, Fig. S6). Pias1 protein levels were significantly reduced in the soluble fraction in both WT and zQ175 males and females at 8 mo with KD (*SI Appendix*, Fig. S7) but insoluble levels were unaltered between groups. Finally, we evaluated accumulation of HMW mHTT. This accumulation was not affected at 8 or 13.5 mo (with the exception of a change in presymptomatic female mice at 13.5 mo), unlike in R6/2 mice where Pias1 aberrantly accumulated in the insoluble fraction and reduction of Pias1 reduced accumulation of HMW mHTT (*SI Appendix*, Figs. S4, S5*E*, and S7) (16).

Presymptomatic Pias1 Knockdown Differentially Modulates the Transcriptional Landscape in WT and zQ175 Mice over Time. Transcriptional dysregulation is an early hallmark of HD pathogenesis (18, 28). Pias1 is a well-established regulator of transcription (29) either through its role as a negative regulator of inflammatory transcriptional response through binding of NF-κB (30–32) or as an E3 SUMO ligase for transcription factors that regulate neuronal transcription, suggesting that Pias1 KD could impact the transcriptional profile in the brain (33–36). We therefore evaluated transcriptional changes in tissue from presymptomatic treated male mice collected at 8 and 13.5 mo on GFP-positive microdissected striatal tissue, time points which parallel evaluation of Pias1 KD.

Eight months of age. Four conditions were assessed: WT miSafe, WT miPias1.3, Het zQ175 miSafe, and Het zQ175 miPias1.3, with three mice each per condition at 8 mo, profiled by bulk mRNAseq analysis. Principal component analysis (PCA) on the top 500 genes showed little separation associated with genotype (*SI Appendix*, Fig. S8*A*) as described (18). A clear separation associated with treatment in WT animals was observed.

Next, statistical analysis of differentially expressed genes (DEGs) was performed using DEseq2 (37) with a significance threshold of 10% false discovery rate (FDR). A total of 3,332 disease-associated DEGs were observed between WT and zQ175 miSafe-treated animals, 882 DEGs in WT animals with miPias1.3 treatment, and 175 DEGs in zQ175 animals with miPias1.3 treatment (Dataset S2). DEGs were analyzed using Gene Ontology (GO, GOrilla) (38) enrichment to assess specific biological processes, and Ingenuity pathway analysis (IPA) for upstream regulators associated with Pias1 KD (Datasets S3 and S4). Regulation of biological processes, neurogenesis, and regulation of neuron differentiation were impacted in WT animals treated with miPias1.3 (*SI Appendix*, Fig. S8*B*). In zQ175 mice, no significant processes were observed and only intracellular signal transduction was enriched by Pias1 reduction (*SI Appendix*, Fig. S8*C*). IPA upstream analysis in WT-treated animals showed enrichment for regulators including HTT, CREB1, L-dopa, SNCA, and BDNF (*SI Appendix*, Fig. S8*D*). Some of these regulators were also enriched in zQ175 mice with treatment (e.g., CREB1, BDNF, *SI Appendix*, Fig. S8*E*) suggesting some overlap in Pias1 targets.

Of the 175 DEGs dysregulated in zQ175 animals with miPias1.3 treatment, 119 were also dysregulated between control zQ175 and control WT animals, indicating a significant association with disease by Fisher's exact test ($P < 0.0001$, Dataset S5). When analyzing the

effect of miPias1.3 treatment on these 119 genotype-specific DEGs, processing of mRNA was also enriched by GO analysis in the zQ175 animals (*SI Appendix*, Fig. S8*F*). IPA upstream regulator analysis of these genes (119) revealed similar regulators to those detected when all DEGs in zQ175 mice with KD were assessed (*SI Appendix*, Fig. S8*G*) (175). This suggested that Pias1 may regulate a subset of disease-associated transcriptional networks at this age. Supporting this, a significant 92.4% of genes that were altered in expression by miPias1.3 treatment in zQ175 mice were also disease-dysregulated and showed inverse fold changes (FCs) with Pias1 KD, representing a normalizing effect on aberrant HD-associated transcription at this early time point ($P < 0.0001$, *SI Appendix*, Fig. S8*H*). Together, transcriptional analysis at 8 mo revealed a clear impact of Pias1 KD in both WT and zQ175 mice.

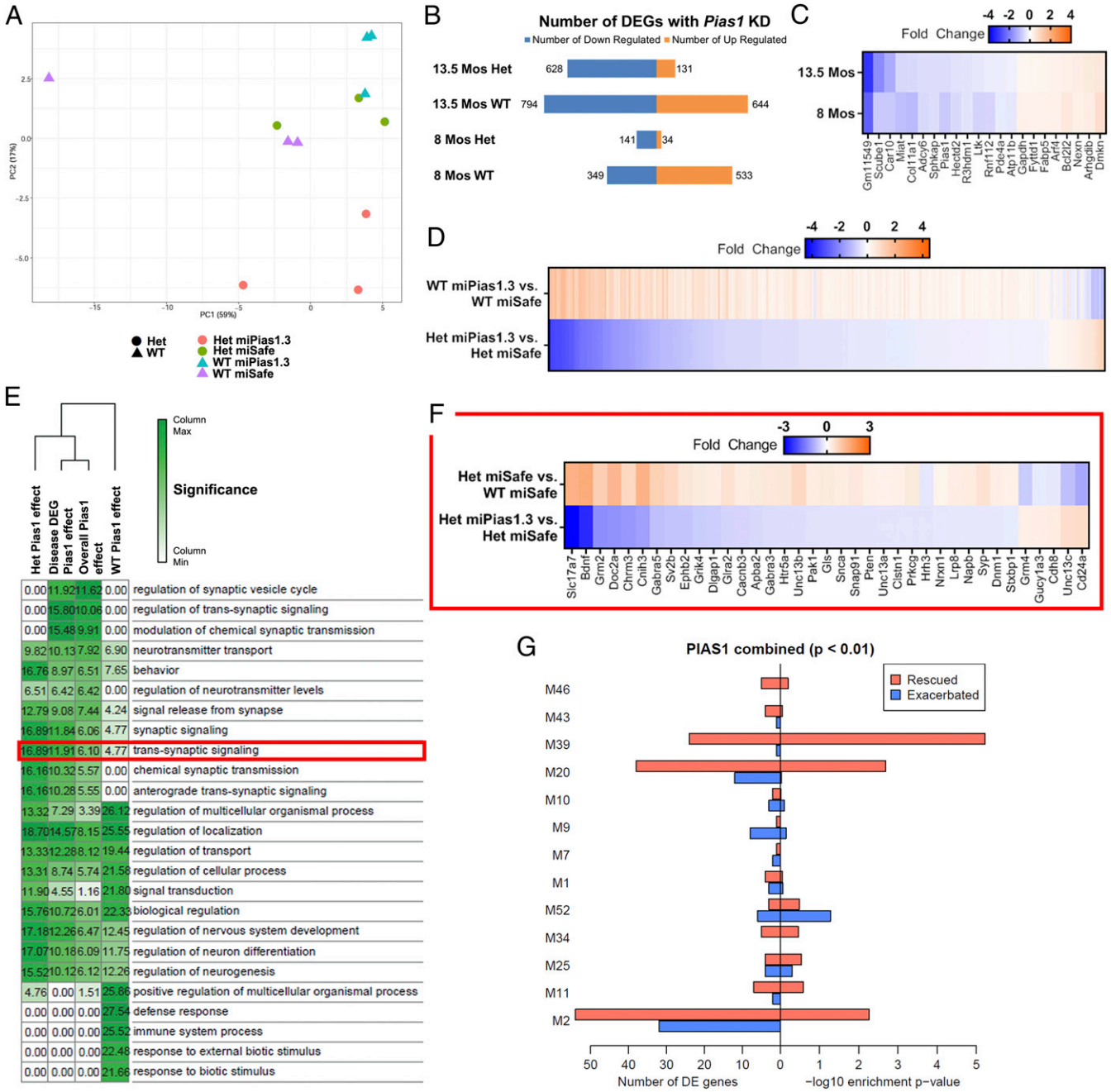

Fig. 1. Presymptomatic Pias1 KD regulates transcription in WT and HD mice at 13.5 mo of age. (*A*) PCA shows separation by both treatment and genotype. (*B*) Barplot showing number of DEGs per contrast at 8 and 13.5 mo with Pias1 KD. (*C*) Fold-change heatmap of 22 shared DEGs between age groups; of these, only Pde4a is a likely off-target DEG as determined by siSPOTR (70, 71) (*SI Appendix*, Table S1). (*D*) Fold-change heatmap of Pias1 KD modulated DEGs in WT and zQ175. (*E*) Heatmap (column min-max transformed log2 adjusted *P* values) and hierarchical clustering of top significantly enriched GO biological processes for WT Pias1 effect (WT miPias1.3 vs. miSafe), Het Pias1 effect (Het miPias1.3 vs. miSafe), overall Pias1 effect (279 genes shared between WT Pias1 effect and Het Pias1 effect), and disease DEG Pias1 effect (521 disease-associated DEGs modulated by miPias1.3 treatment). (*F*) Representative fold-change heatmap of GO process transsynaptic signaling shows inverse fold change of DEGs associated with treatment. (*G*) Bar chart from combined mRNAseq datasets showing the number and significance of rescued and exacerbated genes within disease-associated transcriptional modules originally identified in the allelic series transcriptional data (18). $n = 3$ animals per age per group.

Thirteen and a half months of age. mRNAseq was next carried out on tissue collected at 13.5 mo, when progressive genotype-specific transcriptional changes are more pronounced in zQ175 mice (18) and when a significant reduction in Pias1 transcript was detected (*SI Appendix*, Fig. S5*A*). PCA on the top 500 genes revealed a clear separation between all groups; both genotype and treatment conditions showed distinct separation along PC1 and PC2, representing the maximal variance among samples (Fig. 1*A*) and indicate that reduction of Pias1 has a substantial, and reproducible, impact on gene expression in both HD and WT mice at this time point. DEGs were determined as above (Dataset S2). Overall, WT animals still had a higher number of dysregulated genes with miPias1.3 treatment than zQ175 animals (1,438 for WT and 759 for zQ175, Fig. 1*B*) with 3,288 genes representing disease-associated DEGs (miSafe zQ175 vs. miSafe WT). zQ175 animals treated with miPias1.3 had a larger number of DEGs by 13.5 mo (759 versus 175 at 8 mo). Of these DEGs, there were 22 shared and similarly dysregulated genes between the two age groups for zQ175 mice with miPias1.3 treatment, including Pias1, representing a significant overlap of target genes ($P < 0.0001$, Fig. 1*C*). Of note, there was no miPias1.3 treatment effect on *Htt* expression at either time point, therefore DEGs are not a consequence of altered Htt expression (Dataset S2).

Of the genes dysregulated by Pias1 KD in both WT and zQ175 mice, a significant overlap of 279 DEGs were in common between genotypes ($P < 0.0001$, Fig. 1*D*), with the majority inversely regulated based on genotype, supporting a unique role for Pias1 in the context of mHTT expression. When analyzed by GO, these data revealed top processes related to synaptic vesicle and neurotransmitter release, suggesting that Pias1 is differentially modulating these neuronal functions based on disease context (Fig. 1*E*, column 3, Dataset S3). Remaining DEGs were unique to either WT or zQ175 mice when treated with miPias1.3. These genotype-specific changes were further analyzed by assessing all DEGs mediated by Pias1 KD for each genotype by GO and IPA, with each showing unique enrichment terms (Fig. 1*E*, Datasets S3 and S4, and *SI Appendix*, Fig. S9*A*). In WT animals with Pias1 KD, processes related to cellular defense mechanisms, immune responses, and inhibition of immune-related processes were observed (Fig. 1*E*, column 4, 1*F*), consistent with Pias1's known role in immune function (30–32). zQ175 animals with Pias1 KD showed enrichment for genes involved in cellular communication, neuronal transmission, and development (Fig. 2*E*, column 1) and IPA revealed upstream pathways associated with HTT and neuronal trophic support (*SI Appendix*, Fig. S9*A*). Overall, analysis shows a clear impact in both WT and zQ175 mice but suggests that Pias1 may be differentially mediating pathways in zQ175 mice compared to control animals. In WT animals, networks appear to be centered on immune and cellular defense functions while in zQ175, networks are associated with neuronal function.

We next examined the effect of treatment on disease-specific dysregulated genes at 13.5 mo. A significant overlap of 521 DEGs was observed ($P < 0.0001$) when comparing zQ175 miPias1.3 (Het miPias1.3 vs. miSafe) DEGs to those from control WT and zQ175 animals (Het miSafe vs. WT miSafe, Dataset S5). GO and IPA analysis revealed that Pias1 KD modulated disease-associated gene expression involved in neuronal function and health, including those involved in transsynaptic signaling, synaptic transmission, and nervous system development (Fig. 1*E*, column 2, and *SI Appendix*, Fig. S9*A*). A significant number of these 521 genes showed an inverse fold change when compared to control zQ175 animals ($P < 0.0001$) further suggesting a normalizing effect of Pias1 KD on a subset of disease-associated genes (Fig. 1*F*). Together, transcriptomic profiling of miPias1.3-treated zQ175 animals suggests that Pias1 affects neuronal function in HD mice, and length of KD treatment or stage of disease influences modulation of transcriptional profiles.

Transcriptional analysis by mRNAseq was also carried out in female mice following miPias1.3 treatment. PCA from RNAseq of female mice at 13.5 mo showed separation based on genotype but not treatment (*SI Appendix*, Fig. S10*A*) with fewer DEGs observed in females as compared to males (*SI Appendix*, Fig. S10*B* and Dataset S2). Overall, female mice showed differential expression and impact of Pias1 KD as compared to their male counterparts (*SI Appendix*, Fig. S10). It is not clear why there are sex differences in genes affected by Pias1 KD; these differences remain to be explored (*SI Appendix*). It is noteworthy that the vast majority of transcriptomic studies in R6/2 mice have been carried out in males.

Pias1 KD Rescues Disease-Associated Transcriptional Modules Including DNA Damage. We next compared the male zQ175 transcriptional profiles to a previously established transcriptome from an allelic series derived from zQ175 mice (18) and compared Pias1-associated signatures on defined disease-associated profiles. Allelic series transcriptional changes correspond with gene changes found in human HD brain (18, 28). For this analysis, the combined data from both the 13.5- and 8-mo-old presymptomatic KD cohorts were compared to RNAseq data from the zQ175 allelic series. First, we looked at gene expression changes between zQ175 and WT in our miSafe, control treatment groups; a scatterplot of Z scores calculated using the log2FC from each dataset showed strong concordance with previously established transcriptional dysregulation ($R = 0.72$, $P < 0.0001$) (*SI Appendix*, Fig. S9*B*). To assess the impact of Pias1 KD per a genotype, we employed the same scatterplot and correlation analysis comparing zQ175 treatment effect against the WT treatment effect. A significant, negative concordance was observed ($R = -0.02$, $P < 0.05$), further supporting a disease-specific function and impact of Pias1 modulation in HD (*SI Appendix*, Fig. S9*C*).

To determine the impact of miPias1.3 treatment on previously established, disease-associated gene networks, our datasets were analyzed against disease correlated coexpression modules identified in the allelic series (18). DEGs associated with KD of Pias1, that also showed inverse fold change from previously observed directional expression related to increasing CAG length, were significantly overrepresented within M20 and M39 modules, highly enriched for those within M2, and modestly but not significantly enriched in others (M11, M25, M34, M1, M10, M43, and M46). Significant overrepresentation in M20 and M39 modules suggests a rescue of these HD-associated transcriptional profile. Slight but not significant exacerbations for genes enriched in M52, M10, M7, and M9 modules were also observed (Fig. 1*G* and Dataset S6).

M20 and M39 modules are enriched for genes related to DDR signaling (18) and the specific genes contributing to the significant overrepresentation in both modules with Pias1 KD suggest a functional impact on intra and extracellular signaling, cellular division, and neuronal growth in zQ175 mice (Dataset S6). Therefore, rescued genes associated with these modules suggest either an indirect role for Pias1 in regulating DDR pathways, e.g., through p53 signaling and ubiquitination pathways, or a direct impact on modulating gene networks associated with these mechanisms. Indeed, PIAS1 has been previously defined to modulate DDR pathways and p53 through SUMOylation (10, 23, 39). Since M2 is enriched with MSN identity genes that are down-regulated with mHTT CAG expansion, the enrichment of Pias1 KD rescued genes in this module consistently suggests neuroprotective effects of Pias1 reduction in striatal MSNs of HD mice.

The remaining coexpression modules that are modestly rescued by Pias1 KD are enriched for genes involved in synaptic function and HD-associated pathways (Dataset S6). The slightly exacerbated M52 module confirms the negative regulatory role of Pias1 in modulating NF-κB inflammatory pathways, with KD potentially further activating this module (30). Our data for

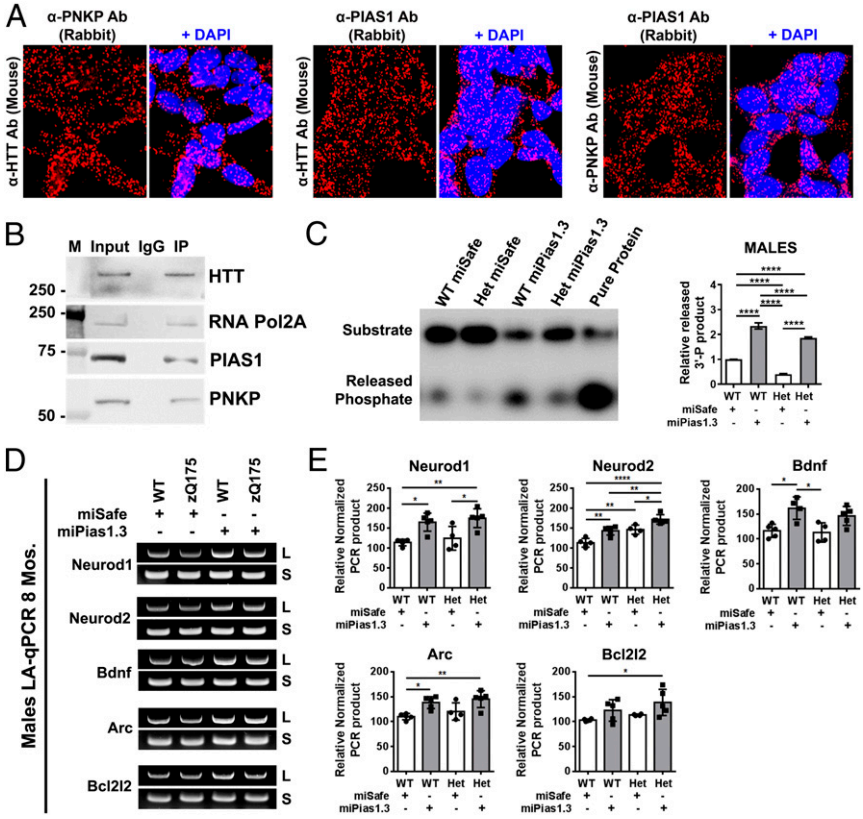

Fig. 2. Pias1 is part of the TCR complex and KD affects DNA damage repair in zQ175 mice. (*A*) PLA in SY5Y cells with PNKP, HTT, and PIAS1 antibodies. (*B*) Coimmunoprecipitation of the nuclear extract from SY5Y cells with HTT antibody. (*C*) mHTT-perturbed enzymatic activity of repair enzyme PNKP in the striatum is rescued with Pias1 KD in zQ175 mice ($n = 3$). (*D*) LA-qPCR of normalized transcriptional targets in males at 8 mo ($n = 4$ to 5/group) and (*E*) quantification of PCR products. *Neurod1*: treatment, $F_{1,\ 15} = 25.110$, $P < 0.001$, $F_{1,\ 15} = 1.011$, $P > 0.05$, *Neurod2*: treatment, $F_{1,\ 15} = 29.000$, $P < 0.0001$, genotype, $F_{1,\ 15} = 35.460$, $P < 0.0001$, *Bdnf*: treatment, $F_{1,\ 14} = 19.970$, $P < 0.001$, genotype, $F_{1,\ 14} = 1.152$, $P > 0.05$, *Arc*: treatment, $F_{1,\ 15} = 17.89$, $P < 0.001$, genotype, $F_{1,\ 15} = 1.897$, $P > 0.05$, *Bcl2l2*: treatment, $F_{1,\ 15} = 7.636$, $P < 0.05$, genotype, $F_{1,\ 15} = 2.694$, $P < 0.05$. Long amplicon (L) normalized to short amplicon (S). $*P < 0.05$, $**P < 0.01$, $****P < 0.0001$, ns = not significant, values represent means ± SEM and individual values.

disease-associated effects highly correlate with previously published zQ175 transcriptional data and the analysis revealed a significant impact on disease-associated DDR gene networks with Pias1 modulation in HD.

PIAS1 Is Part of the TCR Complex along with HTT and Modulates PNKP Activity and Genomic Stability In Vivo. We previously showed that PIAS1 and HTT interact (15) and that KD of PIAS1 modulated HD-associated molecular readouts in R6/2 mice, suggesting a functional association between PIAS1 and HTT in the brain (15, 16). Here we show that Pias1 KD modulated DDR transcriptional coexpression modules in our zQ175 mice. HTT was recently identified as a member of the TCR complex together with PNKP and RNA Pol2A, with mHTT reducing PNKP activity and genomic stability (19). Therefore, we examined whether PIAS1 is also part of the TCR complex, given its ability to interact with HTT (15). Endogenous HTT was coimmunoprecipitated from nuclear extracts of human SH-SY5Y neuroblastoma cells and the precipitated complex was analyzed by Western blot and interactions were confirmed by proximity ligation assay (PLA). PIAS1 was coprecipitated with HTT along with PNKP and RNA Pol2A, and colocalized with PNKP and HTT by PLA, suggesting that PIAS1 is a component of the TCR complex in neuronal-like cells (Fig. 2 *A* and *B* and *SI Appendix*, Fig. S11*A*).

We next analyzed enzymatic activity of Pnkp in vivo. Activity was assessed using 32P-labeled 3′-phosphate-containing oligo substrate and Pnkp-containing tissue lysates from GFP^+ regions of 8-mo WT and zQ175 males treated with miSafe or miPias1.3, presymptomatically. HD animals recapitulated reduced enzymatic activity of Pnkp (19), and miPias1.3 treatment rescued this perturbed activity (genotype: $F_{1,\ 8} = 208.0$, $P < 0.0001$; treatment: $F_{1,\ 8} = 1{,}402$, $P < 0.0001$, Fig. 2*C*). An increase in activity in WT animals with treatment was also observed.

PNKP is critical for maintaining genomic integrity in the brain (40). A decrease in enzymatic activity of Pnkp in zQ175 mice corresponds with decreased integrity of actively transcribing genes, including *Neurod1* and *Neurod2* at 7 wk of age (19). To test whether Pias1 KD may increase genomic integrity of transcriptionally regulated genes, we selected several candidate genes (*Neurod1*, *Neurod2*, *Bdnf*, *Arc*, and *Bcl2l2*) that were regulated by Pias1 KD in males at either or both 8 mo, when we observed rescue of Pnkp activity, and 13.5 mo (Dataset S2) and assessed their integrity using long-amplification qPCR (LA-qPCR) as described (22, 41). LA-qPCR assesses stability through quantification of long genomic DNA amplicons, with regions harboring more damage having decreased polymerase amplification efficiency. For all five genes at 8 mo, miPias1.3 treatment showed a significant treatment effect by LA-qPCR in males, suggesting an increase in genomic integrity of these genes (Fig. 2 *D* and *E*). Interestingly, for female mice, Pias1 KD only significantly impacted genomic integrity for *Neurod2* (*SI Appendix*, Fig. S11 *B* and *C*), suggesting a differential impact on stability based on genotype in females. Post hoc analysis failed to reveal the source of this significance. Differences in genomic stability of these genes may be related to observed differences at the expression level for these genes between males and females (Fig. 1, *SI Appendix*, Fig. S10, and Dataset S2). Together,

data strongly suggests that Pias1 is modulating genomic stability in vivo in male mice, potentially stabilizing genes contributing to neuronal health and function, consistent with the gene expression profiles.

Finally, we evaluated Pnkp protein levels using Western blot analysis on striatal tissues from all cohorts of zQ175 presymptomatic- and symptomatic-treated animals using an antibody previously validated to detect mouse Pnkp in brain (40). Pnkp was detected in the soluble fraction only and no modulation of Pnkp abundance was detected (*SI Appendix*, Fig. S11 *D–I*). This suggested an alternative form of modulatory activity for Pias1 on Pnkp versus altered abundance.

PIAS1 Is a SUMO E3 Ligase for PNKP. A possible mechanism through which PIAS1 may modulate PNKP activity is via PIAS1's function as an E3 SUMO ligase (*SI Appendix*, Fig. S12*A*) and a recent proteomics screen assessing SUMOylated protein substrates identified PNKP as a SUMO target (42). Therefore, we searched for SUMOylation consensus sites (ψKXE, where ψ is a hydrophobic amino acid) within PNKP (43) using SUMOplot (Abcepta). Several probable SUMO consensus motifs (11 total) were identified in both the N and C terminus of human PNKP (*SI Appendix*, Fig. S12*B*). Many of these lysines are highly conserved in mammals and lower vertebrates (*SI Appendix*, Fig. S12*C*), suggesting that PNKP SUMOylation may have an important evolutionary contribution to PNKP function.

To test PNKP SUMOylation, a cell-based SUMOylation assay was used as described (15). Myc-tagged PNKP cDNA was coexpressed with either His-SUMO1 or His-SUMO2 constructs in HeLa cells. Lysates were processed using His purification under denaturing conditions and protein analyzed by Western blotting for predicted motility shift of modified substrate. PNKP is SUMOylated by SUMO1 by at least two SUMO moieties as observed by a predicted mobility shift detected by both anti-PNKP and anti-Myc antibodies (*SI Appendix*, Fig. S13*A*). Additional laddering at higher molecular weights suggests further polySUMOylation or subsequent polyubiquitylation. His-SUMO2 similarly demonstrated PNKP SUMOylation and subsequent higher molecular weight laddering (Fig. 3*A* and *SI Appendix*, Fig. S13*B*). Together with computational data and previously reported proteomics data (42), the in-cell SUMOylation data support PNKP as a bona fide SUMO substrate.

Since PNKP is a substrate for SUMOylation, we next tested whether PIAS1 might serve as a SUMO E3 ligase for PNKP. First, the interaction between PIAS1 and PNKP was confirmed in HeLa cells used for the SUMOylation assay by coimmunoprecipitation (*SI Appendix*, Fig. S14*A*). Second, to assess if PIAS1 modulates PNKP SUMOylation, in-cell SUMOylation assays were carried out in the presence of increased or decreased PIAS1. PIAS1 siRNA was cotransfected with Myc-PNKP and His-SUMO2, causing a significant decrease in PNKP SUMOylation as determined by a size shift reflective of two SUMO2 moieties ($P < 0.01$, Fig. 3*B*). Third, PIAS1 overexpression under SUMO-limiting conditions was also assessed. To detect enhanced SUMOylated PNKP by PIAS1, Myc-PNKP was coexpressed with PIAS1 in HeLa cells with limiting His-SUMO2 to reduce baseline levels of SUMOylated PNKP, resulting in a significant increase in PNKP SUMOylation with PIAS1 overexpression (1xSUMO $F_{2,\ 6} = 14.60$, $P < 0.05$; 2xSUMO $F_{2,\ 6} = 10.90$, $P < 0.05$, Fig. 3*C*). Experiments were repeated using His-SUMO1 with similar results (*SI Appendix*, Fig. S14 *B* and *C*). Together, these data support PIAS1 as a probable E3 ligase for PNKP by both SUMO1 and SUMO2.

PIAS1 Reduction in Control and HD iPSCs Modulates Transcription and Increases PNKP Activity. To investigate the impact of PIAS1 in HD human neurons, reduction of PIAS1 was first carried out by treating multiple human iPSC control and HD lines (CS71iCTR20n6 [20Q], CS83iCTR33n1 [33Q], CS25iCTR18n6 [18Q], CS14iCTR28n6 [28Q], CS02iHD66n4 [66Q], CS81iHD71n3 [71Q] (44) and CS09iHD109n4 [109Q] (45) with siRNA against PIAS1 via lipid nanoparticles to determine whether similar transcriptional changes are induced by PIAS1 reduction as observed in zQ175 mice. This method of delivery improves transfection efficiency in hard to transfect cells with transfection apparent in nearly all cells at one day after a single treatment (day 19, *SI Appendix*, Fig. S15*A*). iPSCs were further differentiated to pure neurons with striatal characteristics as described (44, 45) and mRNAseq carried out at day 37, with a significant reduction of PIAS1 observed with some variability across lines (*SI Appendix*, Fig. S15*B*). PCA of global gene expression showed variation occurred from human patient variation rather than genotype or treatment (*SI Appendix*, Fig. S15*C*). A limited number of DEGs were observed in HD versus control (Fig. 4*A* and Dataset S7) using this differentiation method. However, a significant PIAS1 effect was observed in both control and HD lines (Fig. 4*A* and Dataset S7) with a large overlap in the DEGs between control and HD samples (Fig. 4*B*). Specifically, 2,228 overlapping DEGs were observed in both control and HD neurons which changed in the same direction. GO analysis on the DEGs generated from control neurons following PIAS1 KD showed enrichment of signaling pathways including EIF2, axonal guidance, and CREB signaling (Fig. 4*D*). In HD lines, significant enrichment in terms related to synaptic signaling and transmission were observed (Fig. 4*E*). IPA analysis predicted activation of BDNF in both control and HD neurons following PIAS1 KD (*SI Appendix*, Fig. S15*D*) similar to transcriptional analysis above for mice (*SI Appendix*, Figs. S8 and S9). IPA analysis enriched for CREB signaling and the dopamine-DARPP32 feedback in cAMP signaling in HD neurons which each play an important role in MSN action potential processing (46). Finally, we compared PIAS1-associated DEGs to coexpression modules M2, M20, and M39 that had significant overrepresentation in DEGs associated with Pias1 KD in zQ715 mice (Figs. 1*G* and 4 *F–G*). Hypergeometric test for numbers of DEGs and number of genes within these modules revealed a significant overlap with M2 and M39, but not M20 in control and HD neurons (Fig. 4 *F* and *G*, CTRvsM2 $P = 8.06E\text{-}09$, CTRvsM20 $P = 0.488$, CTRvsM39 $P = 5.69E\text{-}05$, HDvsM2 $P = 4.31E\text{-}17$, HDvsM20 $P = 0.252$, and HDvsM39 $P = 6.77E\text{-}05$), supporting an impact for PIAS1 reduction on both DNA damage repair and HD-associated changes.

To more deeply investigate the molecular consequences of PIAS1 reduction in iPSC neurons and mechanisms involved, we used CRISPR-Cas9 genome editing to create an in-del in the PIAS1 locus of a control iPSC line and HD line (33Q and 66Q), to mimic heterozygous loss of function (LOF) in a controlled manner (*SI Appendix*, Figs. S16 and S17). Mutant HTT perturbs PNKP enzymatic activity in iPSC-derived MSNs (19); therefore, we investigated whether activity was altered in the CRISPR-edited PIAS1 KD iPSC-derived MSNs. Nuclear PNKP activity was increased in both the control (33Q) and HD (66Q) iPSC-derived neurons with PIAS1 KD (Fig. 5*A*). In the presence of an expanded polyQ in the 66Q line, PIAS1 KD restored PNKP activity to almost control levels (genotype: $F_{1,\ 8} = 648.7$, $P < 0.0001$; treatment: $F_{1,\ 8} = 5758$, $P < 0.0001$).

We next assessed genomic integrity of several genes impacted by Pias1 KD in vivo as well as mitochondrial DNA as PNKP also functions to repair mitochondrial DNA (47). LA-qPCR was performed as above using human specific primers for target genes on genomic DNA (Fig. 5*B*) and mitochondrial DNA (Fig. 5*C*) harvested from PIAS1 KD neurons. A significant knockdown effect leading to an increase in genomic integrity was detected for *NEUROD1* ($F_{1,\ 8} = 78.64$, $P < 0.00001$). For *BCL2L2* and *BDNF*, significant interactions were detected in HD cells only, suggesting an increase in genomic integrity in that context (*BCL2l2*: $F_{1,\ 8} = 23.73$, $P < 0.01$; *BDNF*: $F_{1,\ 8} = 9.99$, $P < 0.05$). Significant interaction ($F_{1,\ 8} = 7.92$, $P < 0.05$) and knockdown effects ($F_{1,\ 8} = 45.49$, $P < 0.0001$) were also detected

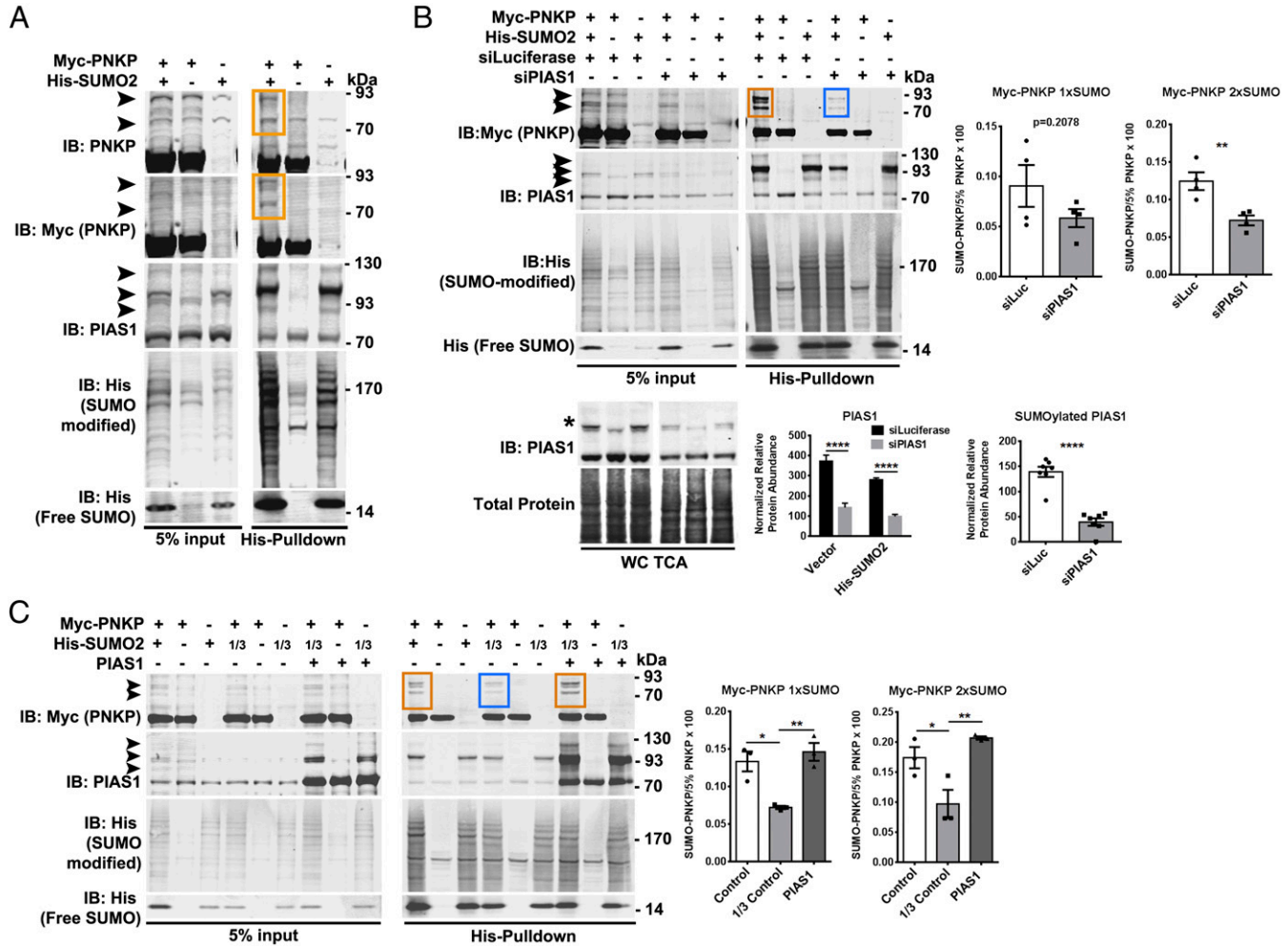

Fig. 3. SUMO2 PNKP modification is mediated by PIAS1 in vitro. (*A*) In-cell, HeLa SUMOylation assay shows PNKP is SUMOylated by SUMO2. Black arrowheads indicate corresponding molecular weight shift of SUMOylated substrate by addition of SUMO moieties (orange boxes). SUMOylated PIAS1 serves as a positive control. (*B*) Significant KD ($P < 0.0001$) of PIAS1 with siRNA (siPIAS1) shows a reduction in SUMOylated PNKP by His-SUMO2 (blue box). Asterisk represents SUMOylated PIAS1 used for quantification ($n = 4$). (*C*) Under SUMO-limiting conditions (1/3 normal input, blue box), PIAS1 overexpression significantly increases PNKP SUMOylation by His-SUMO2 ($n = 3$, orange box). *$P < 0.05$, **$P < 0.01$, ****$P < 0.0001$, ns = not significant, values represent means ± SEM and individual values.

for mitochondrial DNA, indicating an increase in integrity with reduced PIAS1, specifically for HD-iPSC-derived MSNs. Together, the positive impact of PIAS1 KD on PNKP enzymatic activity and integrity of genomic material suggests that PIAS1 is contributing to the TCR response to DNA damage in human neurons.

mHTT May Influence PNKP SUMOylation. Finally, to assess if the presence of the expanded CAG repeat in HTT impacts PNKP SUMOylation and if PNKP is SUMOylated endogenously, protein extracts from iPSC-derived MSNs were generated and evaluated using a coimmunoprecipitation assay capturing endogenous SUMO2/3-modified proteins (Fig. 5*D*). Cells were treated with 50 μM of inhibitor PR619 to prevent deSUMOylation and plus or minus 200 μM hydrogen peroxide prior to harvest to additionally assess if inducing DNA damage impacted PNKP SUMOylation. However, assessment of damage levels by marker γH2AX indicated that hydrogen peroxide treatment did not increase damage levels in this setting (Fig. 5*D*), therefore treated samples were considered as biological replicates for analysis. Immunoblots of PNKP following coimmunoprecipitation of SUMO-2/3-ylated proteins from iPSC-neurons showed high-molecular weight bands that were PNKP immunoreactive, consistent with endogenous PNKP SUMOylation in human neurons (Fig. 5*D*). This signal appeared higher in HD 66Q neurons, suggesting that the presence of expanded mHTT increased PNKP SUMOylation, which was then decreased by PIAS1 reduction. It is therefore possible that PIAS1 is modulating endogenous PNKP SUMOylaton in neurons, with KD restoring mHTT-mediated aberrant SUMOylation; however, additional studies will need to be carried out to confirm this effect. Endogenous SUMOylated PIAS1 was also detected in SUMO-2/3 coimmunoprecipitation with a general increase in both unmodified and SUMOylated PIAS1 in HD iPSC-derived neurons compared to control, suggesting an aberrant increase in PIAS1 in HD neurons. Importantly, an overall accumulation in SUMOylated proteins was observed in HD 66Q neurons compared to control 33Q neurons, which returned closer to normal levels upon PIAS1 reduction. Altogether, these findings suggest that: PNKP is endogenously SUMOylated, this SUMOylation may be modulated by PIAS1 in neurons, and there may be aberrant SUMOylation in the presence of full-length mHTT.

Discussion

Here we provide evidence that PIAS1 KD impacts DDR mechanisms in HD systems potentially through effects on disease-associated transcriptional dysregulation, increasing PNKP activity, restoring TCR activity, and modulating genomic stability. Aberrant

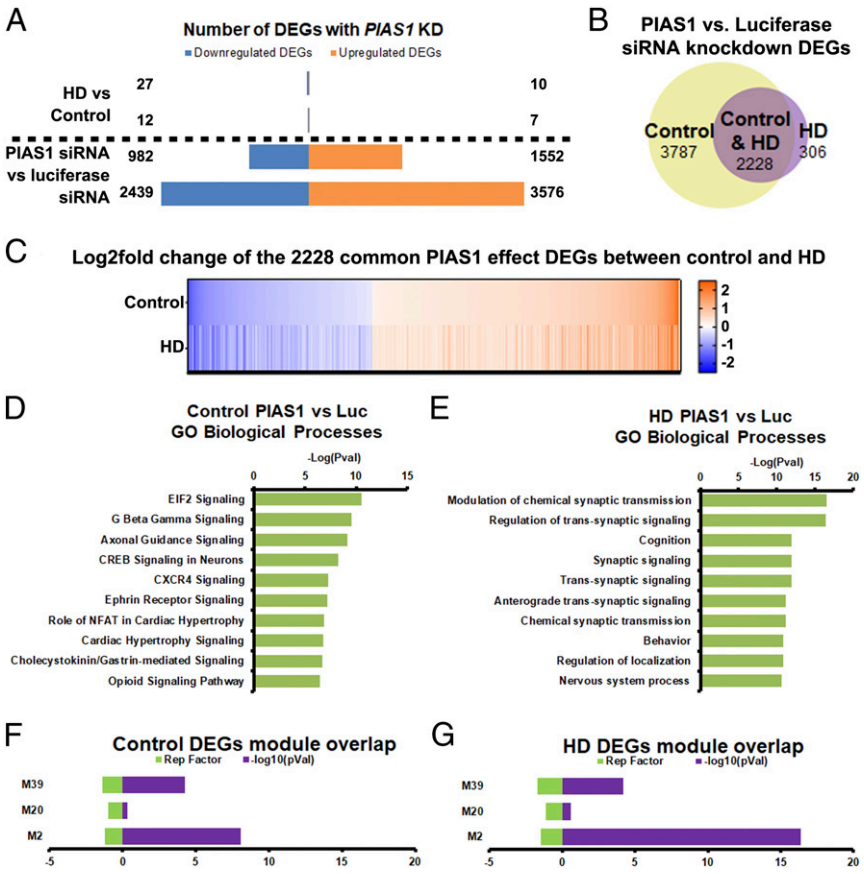

Fig. 4. Neuronal KD of PIAS1 in iPSC derived neurons mRNAseq. (*A*) Barplot showing number of DEGs per contrast. (*B*) Venn diagram showing the DEGs with and without PIAS1 KD shows a majority overlap between control and HD as a result of PIAS1 KD. (*C*) Fold-change heatmap of the 2,228 shared DEGs between control and HD. The top 10 significantly enriched GO biological processes for (D) control samples generated from the PIAS1 KD DEGs and (*E*) for HD samples generated from the PIAS1 KD DEGs. (*F*) Hypergeometric analysis of the siPIAS1 vs. siLuciferase DEGs in control iPSC-derived neurons shows a significant overlap of genes in the M2 and M39 modules, but not M20 module. (*G*) Hypergeometric analysis of the siPIAS1 vs. siLuciferase DEGs in HD iPSC-derived neurons shows a significant overlap of DEGs with the M2 and M39 modules, but not M20 module. Modules are from ref. 18.

DDR is implicated as both an underlying causal factor in neurodegenerative disease (48), and as a disease modifier (49). In HD, DDR mechanisms contribute to variations in age of onset (4–6, 50). HTT itself plays a role in repair mechanisms as a scaffold, including as part of a complex with the repair enzyme PNKP, and we recently reported that mHTT reduces enzymatic activity of PNKP in mouse models of HD and in HD iPSC-derived MSNs (19, 20). Here, we show that PIAS1 is part of a TCR complex through its interaction with HTT and PNKP, that PIAS1 is a SUMO E3 ligase for PNKP and that PIAS1 modulates PNKP activity, both in mouse brain and HD-patient derived neurons. We show that presymptomatic KD of Pias1 in vivo normalized a subset of disease-associated, dysregulated genes in the striatum relating to synaptic function and DDR as well as modulating expression of similar genes in siPIAS1-treated control and HD iPSC neurons. Finally, we show that PNKP may be SUMOylated in neurons endogenously, and this function may be perturbed by HTT polyQ expansion.

In this study, Pias1 KD had little to no impact on mouse behavior or accumulation of HMW mHTT species as we previously observed in the R6/2 model (16); likely due to the subtle behavioral phenotypes in heterozygous zQ715 mice (25, 26, 51, 52) and the lack of insoluble accumulation of Pias1 in zQ175 mouse striatum (*SI Appendix*, *Discussion*). However, in the zQ175 mice, miPias1.3 treatment significantly rescued previously reported transcriptional coexpression modules associated with polyQ length and disease progression (18). Two of these modules (M20 and M39) enrich for DDR signaling and mechanisms, suggesting that Pias1 KD could potentially impact DDR pathways and associated networks. Deficits in DDR mechanisms can lead to decreased genomic integrity in the brain, an effect that is observed in zQ175 mice and HD-patient neurons (19, 48). Pias1 KD increased the genomic integrity of several dysregulated genes whose expression was normalized in male mice, suggesting that deficits in genomic stability may contribute to aberrant transcriptional profiles associated with disease. Therefore, normalized transcriptional profiles may result from genomic stabilization after Pias1 KD. While the impact of this transcriptional normalization on protein levels remains to be assessed, increased genomic integrity may influence overall neuronal health, viability, and neurogenesis (48, 53).

In addition to rescuing DDR transcriptional coexpression modules, Pias1 KD normalized HD-associated transcriptional dysregulation of synaptic-associated biological processes at 13.5 mo, including transsynaptic signaling and modulation of chemical synaptic transmission. Synaptic abnormalities in HD is an early event, with changes preceding neuronal degeneration (54). Synaptic abnormalities are also observed in zQ175 mice (25, 55). This suggests that presymptomatic Pias1 KD normalized disease-associated deficits related to processes regulating synaptic function in the striatum. A significant enrichment of synaptic signaling and transmission terms was also observed upon PIAS1 KD in control and HD iPSC-neurons. Comparison to HD-associated transcriptional modules enriched in Pias1 KD mice showed similar enrichment in siPIAS1 treated iPSC neurons as well, suggesting a conserved mechanism and the potential for PIAS1 reduction

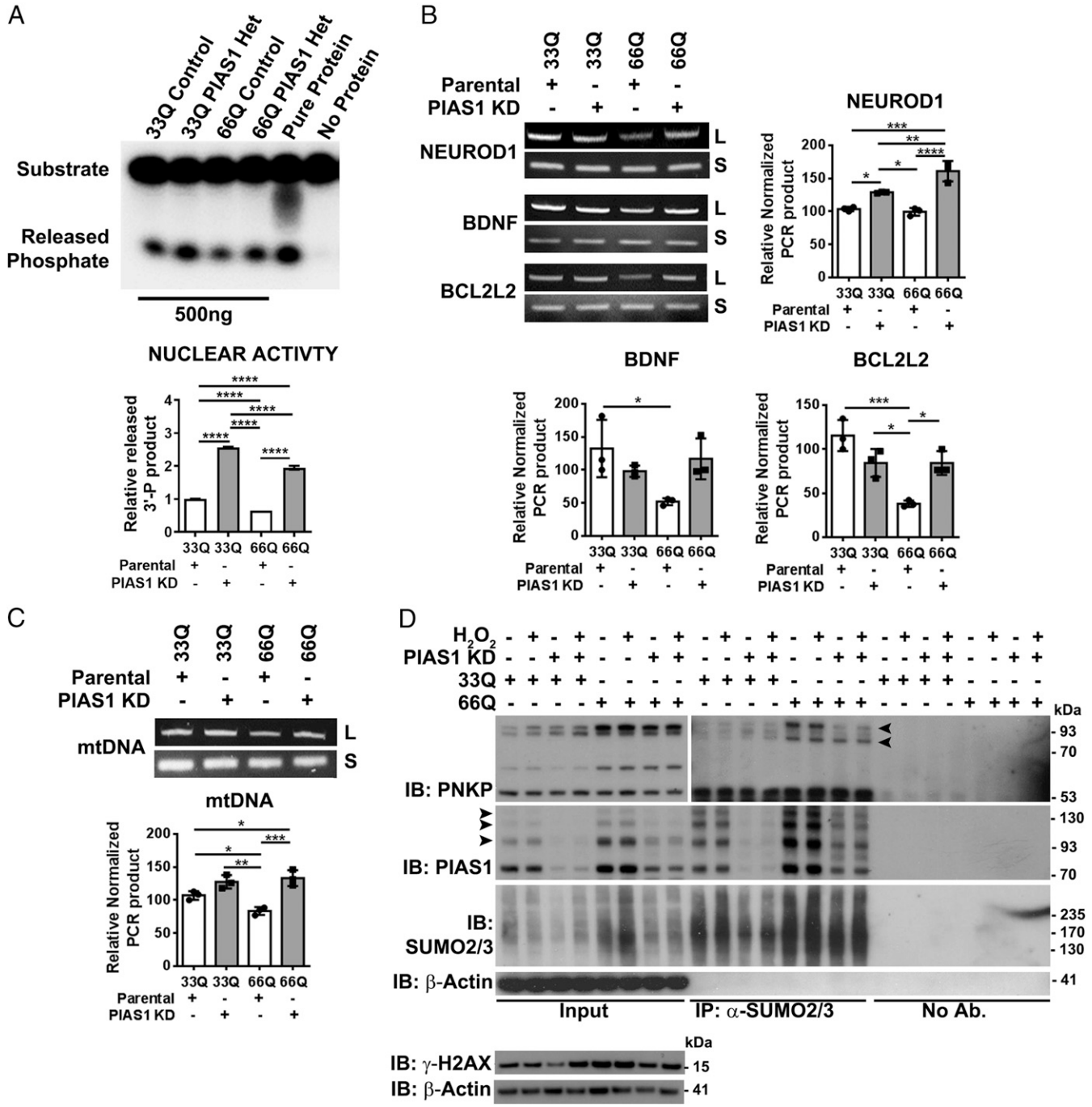

Fig. 5. PIAS1 modulates endogenous PNKP enzymatic activity in iPSC-derived neurons and genomic DNA integrity of key genes is increased. (*A*) Nuclear PNKP activity assay from differentiated neurons ($n = 3$). (*B*) Genomic DNA integrity of key genes is increased with PIAS1 KD ($n = 3$). NEUROD1: treatment, $F_{1,\ 8} = 78.640$, $P < 0.0001$; genotype, $F_{1,\ 8} = 8.246$, $P < 0.05$; interaction, $F_{1,\ 8} = 13.780$, $P < 0.01$, BDNF: treatment, $F_{1,\ 8} = 0.958$, $P > 0.05$; genotype, $F_{1,\ 8} = 3.854$, $P > 0.05$; interaction, $F_{1,\ 8} = 9.992$, $P < 0.05$, BCL2L2: treatment, $F_{1,\ 8} = 0.895$, $P > 0.05$; genotype, $F_{1,\ 8} = 23.700$, $P < 0.01$; interaction, $F_{1,\ 8} = 23.730$, $P < 0.01$. (*C*) Integrity of mitochondrial DNA is increased with PIAS1 KD ($n = 3$): treatment, $F_{1,\ 8} = 45.490$, $P < 0.001$; genotype, $F_{1,\ 8} = 2.963$, $P > 0.05$; interaction, $F_{1,\ 8} = 7.919$, $P < 0.05$. (*D*) SUMO 2/3 coimmunoprecipitation shows endogenous unmodified PNKP and higher molecular weight PNKP immunoreactivity suggesting endogenous PNKP SUMOylation in iPSC-derived neurons ($n = 2$). KD of PIAS1 suggests reduction in high molecular weight PNKP signal. Endogenous SUMOylated PIAS1 served as a control for enrichment of SUMOylated proteins. γH2AX immunostaining suggests no increase in DNA damage levels with H_2O_2 treatment in these cells. Long amplicon (L) normalized to short amplicon (S). $^*P < 0.05$, $^{**}P < 0.01$, $^{***}P < 0.001$, $^{****}P < 0.0001$, ns = not significant, values represent means ± SEM and individual values. β-Actin served as a loading control for whole cell lysate input samples.

to improve HD-associated neuronal dysfunction (Figs. 1*G* and 4 *F* and *G*).

PIAS1 KD also rescued perturbed PNKP enzymatic activity both in vivo and in iPSC-derived neurons, suggesting a modulatory effect for PIAS1 on neuronal TCR. PNKP was previously identified as a SUMO substrate in a proteomics screen (42); however, an assessment of direct SUMO modification or identification of an E3 SUMO ligase had not been described. Here we identify PIAS1 as an E3 SUMO ligase for PNKP in cell culture. PIAS1 and PIAS4 can recruit or evict DDR factors through SUMOylation (10). It is

therefore possible that PIAS1 is recruiting PNKP to the sites of damaged DNA. This may be in conjunction or competition with activation of PNKP through phosphorylation (56) as phosphorylation can prime substrates for SUMOylation (57). However, ubiquitination of PNKP prevents phosphorylation and serves as a degron signal for clearance by the ubiquitin proteasome system (58). Therefore, PIAS1 SUMOylation may be blocking phosphorylation of PNKP similar to reported ubiquitination, serving as a negative regulator of DDR activity or resulting in premature clearance of PNKP (58). Knockdown of PIAS1 may therefore potentially facilitate PNKP phosphorylation and activation. Alternatively, SUMOylation of PNKP could work in collaboration with ubiquitination through SUMO-targeted ubiquitin ligase activity similar to other repair factors at DNA lesions (59–61). Testing the cross-talk between PNKP posttranslational modifications and the protein–protein interactions within DDR complexes will be the focus of future studies.

In humans, genetic modifiers within DDR genes are associated with variations in age of onset and disease progression of HD. In addition to maintaining genomic integrity, these repair mechanisms are linked to CAG repeat instability and somatic repeat expansion (62, 63). Indeed, a HD-associated genetic variant decreasing expression of mismatch repair gene *MSH3* reduced CAG-repeat somatic expansion, delayed onset, and slowed disease progression (4, 7). Further, disease modifier *FAN1*, another nuclease involved in DDR (50, 64), is linked to stabilization of the *HTT* CAG repeat region (65). PIAS1 serves as an E3 SUMO ligase for DDR factors which interact with FAN1 (24). Therefore, modulating DDR pathways through PIAS1 could have an impact on somatic repeat expansion associated with HD progression (66, 67), which will be explored in future studies.

Taken together, we provide a critical mechanistic link between the SUMO system, PIAS1, and DDR in the central nervous system. We provide insight into how DDR pathways and posttranslational modifications might contribute toward disease-associated mechanisms in HD and maintaining genomic instability, with broad implications for HD and other neurodegenerative diseases. Finally, PIAS1 modulation may provide a unique therapeutic target that can normalize key molecular phenotypes in the HD context.

Materials and Methods

For detailed and additional methods, see *SI Appendix, Supplemental Experimental Procedures*.

zQ175 Knockin Mice. Mice were obtained from a CHDI Foundation colony at JAX, bred in house, and maintained on a C57BL/6J background, genotyped, and aged to ∼8 or 13.5 mo in strict accordance with the Guide for the Care and Use of Laboratory Animals of the NIH. Surgeries and behavioral assessments are described in *SI Appendix*.

iPSC Maintenance, PIAS1 siRNA-Mediated Reduction, CRISPR Modification, and Neuronal Differentiation. HD and nondisease repeat iPSCs were generated, differentiated, and characterized as described (44, 45). For PIAS1 siRNA-mediated reduction, iPSC lines were differentiated to neural progenitors (44) and treated with PIAS1 siRNA via lipid nanoparticles (68) (*SI Appendix*). Half media changes were performed on day 18 when PIAS1 or Luciferase (control) siRNA was added to cells at a final concentration of 3.3 μg/mL siRNA and 3 μg/mL ApoE4. CRISPR modification at the PIAS1 locus was performed using the Alt-R CRISPR-CAS9 system from Integrated DNA technologies using manufacturer protocols. Single-cell clone generation was used and successfully edited clones were screened by Western blot and DNA sequencing. Clones with the PIAS1 mutation and the parental lines were differentiated into neurons as described (44).

Western Blot Analysis. Flash-frozen brain tissue was prepared for soluble/insoluble fractionation as described (16). For iPSC CRISPR validation, protein was harvested from frozen cell pellets of the clones using RIPA lysis buffer followed by SDS (sodium dodecyl sulfate) polyacrylamide gel electrophoresis and Western blotting onto nitrocellulose. Membranes were assessed using either infrared fluorescence or chemiluminescence.

mRNASeq. RNA was purified from GFP$^+$ microdissected flash-frozen brain regions or from iPSC-neuron cell pellets (*SI Appendix*). RNA was submitted for mRNAseq as described previously (69). Statistically analysis of differential gene expression was analyzed using DEseq2 (37); a significance threshold was set at a 10% FDR. Enrichment analysis was completed using GOrilla (38) and Ingenuity pathway analysis software. Differential expression analysis of combined data is described in *SI Appendix*. The datasets generated during this study are available at GEO, accession number GSE162349.

PNKP Enzymatic Activity Measurements. The 3′-phosphatase activity of PNKP in the nuclear extract (250 to 500 ng), mitochondrial extract, and purified recombinant His-tagged PNKP (25 fmol) was conducted as described (19). Nuclear extracts for the 3′ phosphatase assay was prepared following standard protocols from cells or mouse brain tissues (19, 22).

Long-Amplification qPCR. Genomic DNA was harvested from GFP$^+$ microdissected striata according to manufacture's protocol using DNeasy Blood & Tissue purification system, omitting vortexing to ensure optimal integrity (Qiagen, 69504). LA-qPCR assays were carried out following an existing protocol (41).

PLA, Coimmunoprecipitation, and Denaturing SUMOylation Assays. PLA experiments were carried out as previously described for SH-SY5Y cells (19). Experimental details for denaturing SUMOylation assay and coimmunoprecipitation experiments for HeLa and iPSC cell lysates are in *SI Appendix*.

Data Availability. RNAseq data have been deposited in GEO (GSE162349) (72). All study data are included in the article and/or supporting information.

ACKNOWLEDGMENTS. We thank Christopher Pearson for his valued insights and input for this study. Primary support was from NIH (NS090390 to L.M.T. and B.L.D.). Additional support was by NIH (NS072453 to J.S.S., NS076631 to B.L.D., NSO79541-01 and R01 EY026089-01A1 to P.S.S., U54 NS091046 NeuroLINCS center to L.M.T.), the Hereditary Disease Foundation (J.S.S. and C.S.-G.), CHDI Foundation (J.S.S.), The Roy J. Carver Trust and The Children's Hospital of Philadelphia Research Institute (B.L.D.), HD CARE (L.M.T.), and an NSF fellowship (E.L.M.). We thank the University of California, Irvine Institute for Memory Impairments and Neurological Disorders and the Optical Biology Shared Resource of the Cancer Center Support Grant (CA-62203) at the UCI for assistance in carrying out experiments. This work was possible, in part, through access to the Genomic High Throughput Facility Shared Resource of the Cancer Center Support Grant (CA-62203) at UCI.

1. The Huntington's Disease Collaborative Research Group, A novel gene containing a trinucleotide repeat that is expanded and unstable on Huntington's disease chromosomes. *Cell* **72**, 971–983 (1993).
2. D. R. Langbehn, R. R. Brinkman, D. Falush, J. S. Paulsen, M. R. Hayden; International Huntington's Disease Collaborative Group, A new model for prediction of the age of onset and penetrance for Huntington's disease based on CAG length. *Clin. Genet.* **65**, 267–277 (2004).
3. N. S. Wexler *et al.*; U.S.-Venezuela Collaborative Research Project, Venezuelan kindreds reveal that genetic and environmental factors modulate Huntington's disease age of onset. *Proc. Natl. Acad. Sci. U.S.A.* **101**, 3498–3503 (2004).
4. M. Flower *et al.*; TRACK-HD Investigators; OPTIMISTIC Consortium, MSH3 modifies somatic instability and disease severity in Huntington's and myotonic dystrophy type 1. *Brain*, awz115 (2019).
5. Genetic Modifiers of Huntington's Disease (GeM-HD) Consortium, Identification of genetic factors that modify clinical onset of Huntington's disease. *Cell* **162**, 516–526 (2015).
6. J. M. Lee *et al.*, A modifier of Huntington's disease onset at the MLH1 locus. *Hum. Mol. Genet.* **26**, 3859–3867 (2017).
7. D. J. H. Moss *et al.*; TRACK-HD investigators; REGISTRY investigators, Identification of genetic variants associated with Huntington's disease progression: A genome-wide association study. *Lancet Neurol.* **16**, 701–711 (2017).
8. J. M. Enserink, Regulation of cellular processes by SUMO: Understudied topics. *Adv. Exp. Med. Biol.* **963**, 89–97 (2017).
9. F. Liebelt, A. C. Vertegaal, Ubiquitin-dependent and independent roles of SUMO in proteostasis. *Am. J. Physiol. Cell Physiol.* **311**, C284–C296 (2016).
10. S. Su, Y. Zhang, P. Liu, Roles of ubiquitination and SUMOylation in DNA damage response. *Curr. Issues Mol. Biol.* **35**, 59–84 (2020).
11. S. Vijayakumaran, D. L. Pountney, SUMOylation, aging and autophagy in neurodegeneration. *Neurotoxicology* **66**, 53–57 (2018).
12. A. Princz, N. Tavernarakis, SUMOylation in neurodegenerative diseases. *Gerontology*, 1–9 (2019).

13. D. B. Anderson, C. A. Zanella, J. M. Henley, H. Cimarosti, Sumoylation: Implications for neurodegenerative diseases. *Adv. Exp. Med. Biol.* **963**, 261–281 (2017).
14. J. S. Steffan *et al*., SUMO modification of Huntingtin and Huntington's disease pathology. *Science* **304**, 100–104 (2004).
15. J. G. O'Rourke *et al*., SUMO-2 and PIAS1 modulate insoluble mutant huntingtin protein accumulation. *Cell Rep.* **4**, 362–375 (2013).
16. J. Ochaba *et al*., PIAS1 regulates mutant huntingtin accumulation and Huntington's disease-associated phenotypes in vivo. *Neuron* **90**, 507–520 (2016).
17. L. B. Menalled *et al*., Comprehensive behavioral and molecular characterization of a new knock-in mouse model of Huntington's disease: zQ175. *PLoS One* **7**, e49838 (2012).
18. P. Langfelder *et al*., Integrated genomics and proteomics define huntingtin CAG length-dependent networks in mice. *Nat. Neurosci.* **19**, 623–633 (2016).
19. R. Gao *et al*., Mutant huntingtin impairs PNKP and ATXN3, disrupting DNA repair and transcription. *eLife* **8**, e42988 (2019).
20. T. Maiuri *et al*., Huntingtin is a scaffolding protein in the ATM oxidative DNA damage response complex. *Hum. Mol. Genet.* **26**, 395–406 (2017).
21. A. Chakraborty *et al*., Neil2-null mice accumulate oxidized DNA bases in the transcriptionally active sequences of the genome and are susceptible to innate inflammation. *J. Biol. Chem.* **290**, 24636–24648 (2015).
22. A. Chakraborty *et al*., Classical non-homologous end-joining pathway utilizes nascent RNA for error-free double-strand break repair of transcribed genes. *Nat. Commun.* **7**, 13049 (2016).
23. Y. Galanty *et al*., Mammalian SUMO E3-ligases PIAS1 and PIAS4 promote responses to DNA double-strand breaks. *Nature* **462**, 935–939 (2009).
24. I. Gibbs-Seymour *et al*., Ubiquitin-SUMO circuitry controls activated fanconi anemia ID complex dosage in response to DNA damage. *Mol. Cell* **57**, 150–164 (2015).
25. T. Heikkinen *et al*., Characterization of neurophysiological and behavioral changes, MRI brain volumetry and 1H MRS in zQ175 knock-in mouse model of Huntington's disease. *PLoS One* **7**, e50717 (2012).
26. B. Zeitler *et al*., Allele-selective transcriptional repression of mutant HTT for the treatment of Huntington's disease. *Nat. Med.* **25**, 1131–1142 (2019).
27. M. P. Mattson, W. Duan, R. Wan, Z. Guo, Prophylactic activation of neuroprotective stress response pathways by dietary and behavioral manipulations. *NeuroRx* **1**, 111–116 (2004).
28. A. Hodges *et al*., Regional and cellular gene expression changes in human Huntington's disease brain. *Hum. Mol. Genet.* **15**, 965–977 (2006).
29. D. Schmidt, S. Müller, PIAS/SUMO: New partners in transcriptional regulation. *Cell. Mol. Life Sci.* **60**, 2561–2574 (2003).
30. B. Liu *et al*., Negative regulation of NF-kappaB signaling by PIAS1. *Mol. Cell. Biol.* **25**, 1113–1123 (2005).
31. B. Liu, K. Shuai, Targeting the PIAS1 SUMO ligase pathway to control inflammation. *Trends Pharmacol. Sci.* **29**, 505–509 (2008).
32. K. Shuai, B. Liu, Regulation of gene-activation pathways by PIAS proteins in the immune system. *Nat. Rev. Immunol.* **5**, 593–605 (2005).
33. S. Grégoire, X. J. Yang, Association with class IIa histone deacetylases upregulates the sumoylation of MEF2 transcription factors. *Mol. Cell. Biol.* **25**, 2273–2287 (2005).
34. C. Riquelme, K. K. Barthel, X. Liu, SUMO-1 modification of MEF2A regulates its transcriptional activity. *J. Cell. Mol. Med.* **10**, 132–144 (2006).
35. D. J. Tai *et al*., MeCP2 SUMOylation rescues Mecp2-mutant-induced behavioural deficits in a mouse model of Rett syndrome. *Nat. Commun.* **7**, 10552 (2016).
36. S. B. Estruch, S. A. Graham, P. Deriziotis, S. E. Fisher, The language-related transcription factor FOXP2 is post-translationally modified with small ubiquitin-like modifiers. *Sci. Rep.* **6**, 20911 (2016).
37. M. I. Love, W. Huber, S. Anders, Moderated estimation of fold change and dispersion for RNA-seq data with DESeq2. *Genome Biol.* **15**, 550 (2014).
38. E. Eden, R. Navon, I. Steinfeld, D. Lipson, Z. Yakhini, GOrilla: A tool for discovery and visualization of enriched GO terms in ranked gene lists. *BMC Bioinformatics* **10**, 48 (2009).
39. T. Kahyo, T. Nishida, H. Yasuda, Involvement of PIAS1 in the sumoylation of tumor suppressor p53. *Mol. Cell* **8**, 713–718 (2001).
40. M. Shimada, L. C. Dumitrache, H. R. Russell, P. J. McKinnon, Polynucleotide kinase-phosphatase enables neurogenesis via multiple DNA repair pathways to maintain genome stability. *EMBO J.* **34**, 2465–2480 (2015).
41. J. H. Santos, J. N. Meyer, B. S. Mandavilli, B. Van Houten, Quantitative PCR-based measurement of nuclear and mitochondrial DNA damage and repair in mammalian cells. *Methods Mol. Biol.* **314**, 183–199 (2006).
42. I. Uzoma *et al*., Global identification of small ubiquitin-related modifier (SUMO) substrates reveals crosstalk between SUMOylation and phosphorylation promotes cell migration. *Mol. Cell. Proteomics* **17**, 871–888 (2018).
43. L. Cappadocia, C. D. Lima, Ubiquitin-like protein conjugation: Structures, chemistry, and mechanism. *Chem. Rev.* **118**, 889–918 (2017).
44. C. Smith-Geater *et al*., Aberrant development corrected in adult-onset Huntington's disease iPSC-derived neuronal cultures via WNT signaling modulation. *Stem Cell Reports* **14**, 406–419 (2020).
45. HD iPSC Consortium, Developmental alterations in Huntington's disease neural cells and pharmacological rescue in cells and mice. *Nat. Neurosci.* **20**, 648–660 (2017).
46. E. Fernandez, R. Schiappa, J. A. Girault, N. Le Novère, DARPP-32 is a robust integrator of dopamine and glutamate signals. *PLOS Comput. Biol.* **2**, e176 (2006).
47. N. Tahbaz, S. Subedi, M. Weinfeld, Role of polynucleotide kinase/phosphatase in mitochondrial DNA repair. *Nucleic Acids Res.* **40**, 3484–3495 (2012).
48. P. J. McKinnon, Genome integrity and disease prevention in the nervous system. *Genes Dev.* **31**, 1180–1194 (2017).
49. T. Maiuri *et al*., DNA damage repair in Huntington's disease and other neurodegenerative diseases. *Neurotherapeutics* **16**, 948–956 (2019).
50. C. Bettencourt *et al*.; SPATAX Network, DNA repair pathways underlie a common genetic mechanism modulating onset in polyglutamine diseases. *Ann. Neurol.* **79**, 983–990 (2016).
51. A. L. Southwell *et al*., An enhanced Q175 knock-in mouse model of Huntington disease with higher mutant huntingtin levels and accelerated disease phenotypes. *Hum. Mol. Genet.* **25**, 3654–3675 (2016).
52. E. A. Spronck *et al*., AAV5-miHTT gene therapy demonstrates sustained huntingtin lowering and functional improvement in Huntington disease mouse models. *Mol. Ther. Methods Clin. Dev.* **13**, 334–343 (2019).
53. H. M. Chow, K. Herrup, Genomic integrity and the ageing brain. *Nat. Rev. Neurosci.* **16**, 672–684 (2015).
54. J. Nithianantharajah, A. J. Hannan, Dysregulation of synaptic proteins, dendritic spine abnormalities and pathological plasticity of synapses as experience-dependent mediators of cognitive and psychiatric symptoms in Huntington's disease. *Neuroscience* **251**, 66–74 (2013).
55. S. Chen *et al*., Altered synaptic vesicle release and Ca^{2+} influx at single presynaptic terminals of cortical neurons in a knock-in mouse model of Huntington's disease. *Front. Mol. Neurosci.* **11**, 478 (2018).
56. H. Segal-Raz *et al*., ATM-mediated phosphorylation of polynucleotide kinase/phosphatase is required for effective DNA double-strand break repair. *EMBO Rep.* **12**, 713–719 (2011).
57. I. A. Hendriks *et al*., Site-specific mapping of the human SUMO proteome reveals co-modification with phosphorylation. *Nat. Struct. Mol. Biol.* **24**, 325–336 (2017).
58. J. L. Parsons *et al*., Phosphorylation of PNKP by ATM prevents its proteasomal degradation and enhances resistance to oxidative stress. *Nucleic Acids Res.* **40**, 11404–11415 (2012).
59. M. H. Tatham *et al*., RNF4 is a poly-SUMO-specific E3 ubiquitin ligase required for arsenic-induced PML degradation. *Nat. Cell Biol.* **10**, 538–546 (2008).
60. Y. Galanty, R. Belotserkovskaya, J. Coates, S. P. Jackson, RNF4, a SUMO-targeted ubiquitin E3 ligase, promotes DNA double-strand break repair. *Genes Dev.* **26**, 1179–1195 (2012).
61. R. Kumar, R. González-Prieto, Z. Xiao, M. Verlaan-de Vries, A. C. O. Vertegaal, The STUbL RNF4 regulates protein group SUMOylation by targeting the SUMO conjugation machinery. *Nat. Commun.* **8**, 1809 (2017).
62. I. V. Kovtun *et al*., OGG1 initiates age-dependent CAG trinucleotide expansion in somatic cells. *Nature* **447**, 447–452 (2007).
63. L. Møllersen *et al*., Neil1 is a genetic modifier of somatic and germline CAG trinucleotide repeat instability in R6/1 mice. *Hum. Mol. Genet.* **21**, 4939–4947 (2012).
64. A. Smogorzewska *et al*., A genetic screen identifies FAN1, a Fanconi anemia-associated nuclease necessary for DNA interstrand crosslink repair. *Mol. Cell* **39**, 36–47 (2010).
65. R. Goold *et al*., FAN1 modifies Huntington's disease progression by stabilizing the expanded HTT CAG repeat. *Hum. Mol. Genet.* **28**, 650–661 (2019).
66. L. Kennedy *et al*., Dramatic tissue-specific mutation length increases are an early molecular event in Huntington disease pathogenesis. *Hum. Mol. Genet.* **12**, 3359–3367 (2003).
67. J. M. Lee, R. M. Pinto, T. Gillis, J. C. St Claire, V. C. Wheeler, Quantification of age-dependent somatic CAG repeat instability in Hdh CAG knock-in mice reveals different expansion dynamics in striatum and liver. *PLoS One* **6**, e23647 (2011).
68. J. A. Kulkarni *et al*., On the formation and morphology of lipid nanoparticles containing ionizable cationic lipids and siRNA. *ACS Nano* **12**, 4787–4795 (2018).
69. A. J. Kedaigle *et al*., Treatment with JQ1, a BET bromodomain inhibitor, is selectively detrimental to R6/2 Huntington's disease mice. *Hum. Mol. Genet.* **29**, 202–215 (2020).
70. R. L. Boudreau, R. M. Spengler, B. L. Davidson, Rational design of therapeutic siRNAs: Minimizing off-targeting potential to improve the safety of RNAi therapy for Huntington's disease. *Mol. Ther.* **19**, 2169–2177 (2011).
71. R. L. Boudreau *et al*., siSPOTR: A tool for designing highly specific and potent siRNAs for human and mouse. *Nucleic Acids Res.* **41**, e9 (2013).
72. R. G. Lim, J. Wu, L. M. Thompson, mRNA sequencing of control and huntington's disease iPSC-derived medium spiny neuron-like cells and Q175 HET or WT mice. Plus and minus knockdown of PIAS1. *Gene Expression Omnibus*. https://www.ncbi.nlm.nih.gov/geo/query/acc.cgi?acc=GSE162349. Deposited 30 November 2020.